PHILOSOPHICAL TRANSACTIONS OF THE ROYAL SOCIETY A MATHEMATICAL, PHYSICAL & ENGINEERING SCIENCES

On Hypersonic Boundary-Layer Interactions and Transition

S. N. Brown, A. F. Khorrami, A. Neish and F. T. Smith

Phil. Trans. R. Soc. Lond. A 1991 **335**, 139-152
doi: 10.1098/rsta.1991.0040

On hypersonic boundary-layer interactions and transition

BY S. N. BROWN, A. F. KHORRAMI, A. NEISH AND F. T. SMITH
Department of Mathematics, University College London, Gower Street, London WC1E 6BT, U.K.

Certain features of recent theoretical research into hypersonic flow are described, concerning boundary layers, shock layers, nozzle flows, wakes, viscous–inviscid interactions, and hypersonic instability and transition. The research is on the continuum range, for high Mach numbers and high Reynolds numbers. The fundamental area of steady, laminar, external planar flows in the hypersonic strong-interaction régime is studied first, for flat-plate and thin airfoils. The interplay of the equally thick viscous and inviscid layers, and the bounding shock, induces global upstream influence of a particularly severe kind, requiring a special computational treatment to determine the flow solution. Secondly, internal steady flow is discussed for a slender hypersonic nozzle configuration which produces a two-stage flow structure downstream of the nozzle throat. Similarities and differences between these external and internal flows are pointed out. Thirdly, properties of instability and transition of the hypersonic boundary layer, its wake and the inviscid outer layer are considered. These include the viscous and the inviscid modes within the viscous boundary layer, inviscid modes within the outer layer, their interaction, vortex-wave interactions, finite-time break-up in the unsteady interactive boundary layer, and surface cooling. Some experimental comparisons, and open problems, are also described.

1. Introduction

Hypersonic boundary layers and shock layers have attracted much scientific and technological interest in the past, and this interest has been renewed in recent years. Boundary-layer effects in particular tend to increase in importance as the Mach number rises, for thin bodies in external flow for example, due to the increase in boundary-layer thickness along with the decreasing slope of the external-flow characteristics and, associated with this, viscous–inviscid interactions come increasingly to the fore. In this article we describe certain aspects of theoretical research into hypersonic flow, in boundary layers, shock layers, nozzle flows, interactions, and their instability and transition properties. Parts of the work are still in progress, and we note in addition that considerations of space necessarily limit the range covered in this article. The research is concerned with the continuum range, for high Mach numbers M_∞ and Reynolds numbers Re, which is a régime of much practical concern. Earlier related work is presented in Stewartson's (1964) book for example, for classical boundary layers, and by Neiland (1970), Werle *et al.* (1973) and Brown *et al.* (1975; see also references therein) for interactive boundary layers.

Phil. Trans. R. Soc. Lond. A (1991) **335**, 139–152
Printed in Great Britain

A convenient starting point is the fundamental area addressed in §2, concerning steady, laminar, external two-dimensional (2D) flows in the hypersonic strong-interaction régime, where the viscous region is comparable in thickness with the main inviscid region, which is bounded by a shock. In contrast with previous investigations on certain limiting cases (in the references above; and in Rizzetta *et al.* 1978; Smith & Gajjar 1983; Brotherton-Ratcliffe 1986; Bowles 1990), analytical features and finite-difference computations are described here for the full interactive formulation, with, for example, fairly general values for γ, the ratio of specific heats, and for the surface temperature. A unique feature is the severity of the upstream-influence factor present, which requires special handling as most of the numerical interactive methods that work successfully for subsonic or supersonic motions fail in the present context. Internal steady flow through a slender hypersonic nozzle is then discussed in §3, with regard to the two-stage flow structure produced (a first stage near the nozzle throat and a second, hypersonic, further downstream) and to the computation of the hypersonic interactive stage. The latter is shock-free and lacks upstream influence, at its outset anyway. Section 4 presents aspects of the instability and transition of the hypersonic boundary layer, its wake and the inviscid shock layer, including viscous and inviscid modes in the compressible boundary layer, inviscid modes in the shock layer, their interaction, surface cooling, and nonlinear effects such as vortex-wave interactions and finite-time break-up in the unsteady interactive boundary layer.

Non-dimensionalized variables are used throughout, namely the velocity components u, v, w, pressure p, density ρ, temperature T, viscosity μ and cartesian coordinates x, y, z. In §§2 and 4 the oncoming free stream has $(u, v, w, p, \rho, T, \mu)$ equal to $(1, 0, 1, 1, 1, 1, 1)$ for an aligned flat plate at $y = 0$ for $0 \leqslant x \leqslant 1$, although other airfoil shapes are also considered there. Section 3 uses a slightly different non-dimensional form more suitable to the nozzle flow studied there. We note in passing that there are various definitions of the term 'hypersonic' in use, but this should become clear in the contexts below. Again, the present work throughout aims to establish the governing parameters of concern and their effects on the hypersonic motions considered.

2. External viscous–inviscid hypersonic flow

This section is used partly to set the scene for the rest of the article. Viscous–inviscid interaction of a strong global kind occurs at Mach numbers M_∞ of the order $Re^{\frac{1}{6}}$, as explained by Stewartson (1964), Neiland (1970) and Brown *et al.* (1975). This is due to the lengthening, with increasing M_∞, of the triple-deck short-scale interaction that governs upstream influence in supersonic boundary layers, along with the thickening proportional to M_∞^2 of the (otherwise $O(Re^{-\frac{1}{2}})$ thick) boundary layer itself and the decrease of the typical external inviscid-influence slope proportional to M_∞^{-1}. As a result, strong interaction in steady hypersonic motion is controlled by a two-layer structure consisting of the boundary layer or viscous shock layer (VSL) next to the body surface and the inviscid shock layer (ISL) lying between the VSL and the relatively thin leading-edge shock. The two layers are comparable in thickness and their properties are mutually dependent.

The typical length scale x is $O(1)$, while the thickness scale y is $O(Re^{-\frac{1}{6}})$, and the interaction parameter taken is the global one,

$$\chi \equiv M_\infty / Re^{\frac{1}{6}}, \tag{2.1}$$

PHILOSOPHICAL TRANSACTIONS OF THE ROYAL SOCIETY A MATHEMATICAL, PHYSICAL & ENGINEERING SCIENCES

which is $O(1)$. In the VSL, the flow solution expands in the form

$$[u, v, p, T, \rho, \mu] \rightarrow [u, \epsilon v, \gamma\chi^3 p, \gamma M_\infty^2 T, \epsilon^2\rho, M_\infty^2 \mu] + \ldots, \tag{2.2}$$

with $\epsilon \equiv \chi^{\frac{3}{2}}/M_\infty$, $y = \epsilon\bar{y}$. Hence the governing equations here are the viscous hypersonic interactive boundary-layer equations,

$$\partial(\rho u)/\partial x + \partial(\rho v)/\partial\bar{y} = 0, \tag{2.3a}$$

$$\rho(u\,\partial u/\partial x + v\,\partial u/\partial\bar{y}) = -p'(x) + (\partial/\partial\bar{y})\,(\mu\,\partial u/\partial\bar{y}), \tag{2.3b}$$

$$\rho\left(u\frac{\partial H}{\partial x} + v\frac{\partial H}{\partial\bar{y}}\right) = \frac{\partial}{\partial\bar{y}}\left(\frac{\mu}{\sigma}\frac{\partial H}{\partial\bar{y}}\right) + \frac{\partial}{\partial\bar{y}}\left\{\left(1 - \frac{1}{\sigma}\right)\mu u\frac{\partial u}{\partial\bar{y}}\right\}, \tag{2.3c}$$

$$p = \rho T, \quad H = \tfrac{1}{2}u^2 + (\gamma p/(\gamma - 1)\,\rho), \quad \mu = \gamma C T, \tag{2.3d, e, f}$$

from the continuity, x-momentum, energy, state, enthalpy and viscosity-law balances respectively. Here $\partial p/\partial\bar{y}$ is zero from the normal momentum balance, and the boundary conditions include

$$u = v = 0, \quad T = T_w, \quad \text{at} \quad \bar{y} = f(x), \tag{2.3g}$$

$$u \rightarrow 1, \quad T \rightarrow 0, \quad \text{as} \quad \bar{y} \rightarrow \delta(x)-. \tag{2.3h}$$

Here (2.3g) describes the case of a prescribed temperature on the given body surface $\bar{y} = f(x)$, with no slip, and (2.3h) produces the merging with the ISL solution outside. Both the pressure $p(x)$ and the VSL displacement shape $\delta(x)$ are unknown functions of x, with δ representing the definite edge of the boundary layer as in (2.3h). Further, C is the constant in the Chapman temperature–viscosity law, which is taken as a fundamental case, and σ is the Prandtl number.

In the ISL, in contrast, hypersonic nonlinear small-disturbance properties hold, with the expressions

$$[u, v, p, \rho] = [1 + \epsilon^2\bar{u}, \epsilon\bar{v}, \gamma\chi^3\bar{p}, \bar{\rho}] + \ldots \tag{2.4}$$

(T is now $O(1)$) producing the nonlinear inviscid equations

$$\partial\bar{\rho}/\partial x + \partial(\bar{\rho}\bar{v})/\partial\bar{y} = 0, \tag{2.5a}$$

$$\bar{\rho}(\partial\bar{v}/\partial x + \bar{v}\,\partial\bar{v}/\partial\bar{y}) = -\partial\bar{p}/\partial\bar{y}, \tag{2.5b}$$

$$\bar{\rho}(\partial\bar{p}/\partial x + \bar{v}\,\partial\bar{p}/\partial\bar{y}) = \gamma\bar{p}(\partial\bar{\rho}/\partial x + \bar{v}\,\partial\bar{\rho}/\partial\bar{y}), \tag{2.5c}$$

for $\bar{p}, \bar{\rho}, \bar{v}$. These are subject to the constraints

$$\bar{v} = \frac{2}{(\gamma+1)}g'\{1 - \chi^{-3}g'^{-2}\} \quad \text{at} \quad \bar{y} = g(x)-, \tag{2.5d}$$

$$\bar{p} = \frac{2}{(\gamma+1)}\left\{g'^2 - \frac{(\gamma-1)}{2\gamma\chi^3}\right\} \quad \text{at} \quad \bar{y} = g(x)-, \tag{2.5e}$$

$$\bar{\rho}\mu = \left(\frac{\gamma+1}{\gamma-1}\right)\left\{1 + \frac{2}{(\gamma-1)}\chi^{-3}g'^{-2}\right\}^{-1} \quad \text{at} \quad \bar{y} = g(x)-, \tag{2.5f}$$

$$\bar{v} = \delta'(x) \quad \text{at} \quad \bar{y} = \delta(x)+, \tag{2.5g}$$

where (2.5d–f) follow from the Rankine–Hugionot conditions, at the unknown shock position $\bar{y} = g(x)$, and (2.5g) is the tangential-flow condition at the unknown ISL–VSL junction.

The main task, then, is to solve (2.3) coupled with (2.5) and to determine the pressure $p(x)$ and the shapes $\delta(x), g(x)$, for prescribed temperature T_w, surface geometry $f(x)$ and hypersonic interaction parameter χ (as well as σ, C). That task is severely hindered by the feature that the viscous–inviscid system (2.3), (2.5) exhibits upstream influence on the global scale, such that the boundary conditions at any $O(1)$ location x downstream can effect the flow properties upstream right to the leading edge $x = 0$. This is because of a free-interaction–branching–departure behaviour present in the near-leading-edge response. That response takes the form (provided $f \leqslant O(x^{\frac{3}{4}})$)

$$p(x) \approx p_0 x^{-\frac{1}{2}} + \ldots + q x^{\alpha - \frac{1}{2}} + \ldots, \tag{2.6a}$$

$$\delta(x) \approx \delta_0 x^{\frac{3}{4}} + \ldots + O(x^{\alpha + \frac{3}{4}}) + \ldots \tag{2.6b}$$

for small positive x, with corresponding series for u, T, ρ, g, etc., starting respectively with the powers zero, zero, $\frac{1}{2}$, $\frac{3}{4}$, etc., while $\bar{y}$ is of order $x^{\frac{3}{4}}$. Here the constants p_0, δ_0 are fixed by the nonlinear leading-order similarity solutions of (2.3), (2.5). The higher-order constant q, however, remains undetermined locally when the power α takes a certain eigenvalue (found from a linear similarity problem). This indeterminacy in q reflects the influence of all the flow conditions further downstream, and indeed q has to be found hand-in-hand with the global solution. Moreover, the eigenvalue α turns out to be large, typically about 30, depending on the surface conditions among other things: see next paragraph. Hence the branching present is a rapid phenomenon of relatively short streamwise scale, at its inception.

Various forward-marching computations of (2.3) with (2.5), or with the tangent-wedge approximation instead, have confirmed the existence of the rapid branching (Werle *et al.* 1973) as have our own computations (see references below), especially when the streamwise step-length is refined. Incidentally, the ultimate form of the free interaction, when allowed to continue nonlinearly, is found to be analogous to the strongly attached singular behaviour analysed in Brown *et al.* (1975) or to the breakaway-separation behaviour of supersonic free interactions as in Stewartson & Williams (1973). We observe also here that very reduced surface temperatures (or values of $\gamma - 1$) and increased body thicknesses are considered by Brown *et al.* (1990), Seddougui *et al.* (1989) (see also references in §1) and by Khorrami & Smith (1991), respectively, in particular regarding upstream influence. Both extremes produce increased α values, the former being connected with the pressure–displacement relation $P = -A$ in standard triple-deck parlance (e.g. see §4 below), while the latter leads to a new pressure-displacement relation, due to the non-uniform solution profiles in the ISL.

An elliptic-type numerical approach is therefore necessary. Our first attempts at this were based on a Carter-like inverse treatment (Carter 1979) in which the displacement shape $\delta(x)$ is guessed for all x, equations (2.3) and (2.5) are both marched forward in x with $\delta(x)$ fixed to yield two $p(x)$ distributions, the change in the $\delta(x)$ distribution is then taken to be proportional to the difference in the two pressures, or rather their gradients (Brotherton-Ratcliffe 1986) and so on. The effect of the downstream conditions can be fed into the treatment in several ways, and similarly for Davis-like treatments (Davis 1984) based on artificial time marching and alternating direction implicit (ADI) or explicit (ADE) sweeping. Unfortunately, another new feature which seems unique to the hypersonic regime then enters and spoils the above treatments, and like-minded ones. It is that even with prescribed displacement (the inverse method) there is still pronounced upstream influence and

PHILOSOPHICAL TRANSACTIONS OF THE ROYAL SOCIETY A MATHEMATICAL, PHYSICAL & ENGINEERING SCIENCES

branching in the system: see references below. This feature contrasts with the supersonic and subsonic régimes and follows from an analysis with δ fixed in (2.6b) which shows the continuing existence of a leading-edge eigenvalue α for the VSL part, and once again the value of α is large. Most other combinations of p, δ treatments likewise yield large eigenvalues; one exception found is where p times δ is prescribed but this has not been followed through as yet. Our corresponding marching schemes for the inverse method and the others above appeared to mirror well the continued presence of the severe branching and hence the failure of such treatments.

Two ways around this extra difficulty were found eventually, after many trials, and these (Khorrami 1991) are summarized below. Both are finite-difference methods based on solving implicitly in the normal direction at successive x stations, which requires inversion of a banded matrix plus a pressure column, one method being essentially a linear sweeping scheme, the other nonlinear. The first uses a global Newton procedure. A global guess is made for all the flow variables, the system (2.3), (2.5) is linearized about that guess, and the resulting linear system for the increments is solved for all x. The branching present now in the linear system can be handled in principle by shooting forward from the leading edge and interpolating linearly to find the correct value of q for the current stage. The increments are then added in, to provide a new global guess, and so the procedure continues. The method is an adaptation of the recent work of Smith & Khorrami (1991) and it works well over relatively short streamwise lengths. Longer-length calculations were done with a modification (which we associate with the Cincinnati school) in which the pressure-gradient term $\mathrm{d}p/\mathrm{d}x$ is forward differenced, effectively suppressing the branching as well as bringing in the upstream influence more directly. The linear system is then swept back and forth through the domain a few times, before the incremental addition is made globally, and so on as above.

The second method, taking its cue from the first, involves a modification of our forward-marching treatment mentioned earlier. Again the VSL pressure gradient (alone) is forward differenced, which suppresses the branching, and, with a global guess for $p(x)$ having been made, the nonlinear system (2.3), (2.5) is swept repeatedly back and forward through the computational domain until the scheme is sufficiently converged. In both methods the Howarth–Dorodnitsyn (HD) transformation is used, as it was in the treatments described earlier, and the condition

$$p \to \gamma^{-1}\chi^{-3} \quad \text{as} \quad x \to \infty, \tag{2.7}$$

associated with the quasi-supersonic flow and hence straight shock far downstream, is accommodated during the sweeping.

Typical grid sizes used were 201×0.1 in x, 101×0.1 in y^*, where y^* is the HD coordinate, and 201×0.005 in η where $\eta = (\bar{y} - \delta(x))/(g(x) - \delta(x))$ acts as the ISLs normal coordinate. Sample results are shown in figure 1. Other details and other solutions are described by Khorrami (1991) and Khorrami & Smith (1991). These appear to be the first such solutions for hypersonic strongly interactive flow, and they have been obtained for the semi-infinite flat plate, for the finite flat plate, for thin bodies ($f \not\equiv 0$ in (2.3g)) and for streamwise concentrated disturbances. Some further analysis has also been carried out for thicker-body flows and for flows on cooled surfaces, as mentioned earlier, and there are many other interesting aspects to be explored.

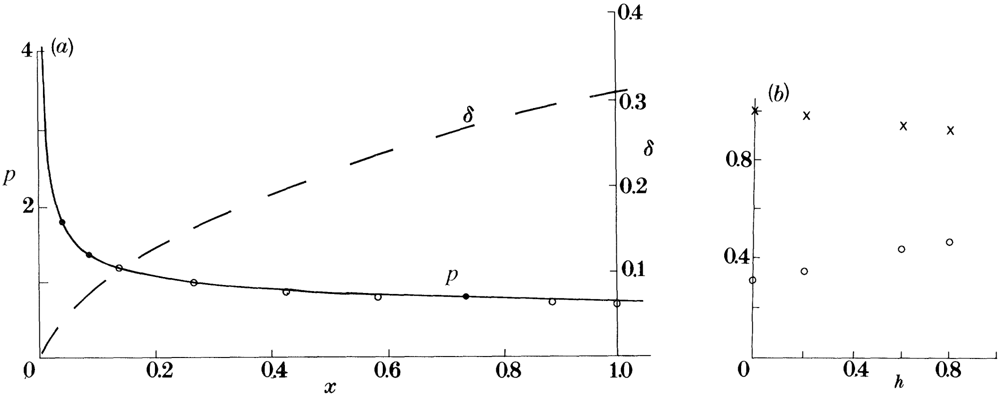

Figure 1. Hypersonic interaction (ISL–VSL) in external flows. (a) The surface pressure p and VSL thickness δ, against x, on a semi-infinite flat plate (solid curve for $\sigma = 1$, solid circles for $\sigma = 0.072$) and on a finite flat plate (open circles, for $\sigma = 1$) with trailing edge at $x = 1$. Here the wall enthalpy is 0.3, the hypersonic parameter $\chi = 1$, and the Chapman constant $C = 1$. (b) Results for non-zero airfoil thickness $f(x) = hx/(1+5x^2)$. ×, $p_w(h)$ at $x = 1$; ○, scaled VSL thickness. From Khorrami (1991) and Khorrami & Smith (1991).

3. Internal hypersonic nozzle flow

The nozzle flow considered here starts from a reservoir upstream, passes through a narrow throat and then expands gradually downstream to become hypersonic. There are two main stages to the flow, the near-throat stage and the farfield stage; the practical interest which set off this theoretical research (by A.N. and F.T.S.) is mostly in the substantial boundary-layer effects that become active in the farfield stage.

In the near-throat stage, the compressible boundary layer remains relatively thin and attached, driven by the inviscid slip velocity. The inviscid solution here, with a 2D assumption made as a starting point, takes the form

$$[u, v, p, \rho, \psi] \to [u, \beta\hat{v}, p, \rho, \psi], \quad [x, y] \to [\beta^{-1}\hat{x}, y] \tag{3.1}$$

for a slender nozzle with typical small slope β, and so the classical thin-layer version

$$(\rho u)_{\hat{x}} + (\rho\hat{v})_y = 0, \quad \rho(uu_{\hat{x}} + \hat{v}u_y) = -p'(\hat{x}), \tag{3.2a, b}$$

$$p/\rho^\gamma = F(\psi) = \text{const.}, \tag{3.2c}$$

holds. This is subject to the mass-flow constraints $\psi = 0, 1$ at $y = -S, 0$, say, where S gives the normalized nozzle shape (with throat width 1), and hence (3.2) gives $2S^2/(\gamma-1) = \rho^{-2}(a_1^2 - \gamma K\rho^{\gamma-1})^{-1}$, to determine $\rho(\hat{x})$ and so on. Here a_1, K are constants. Downstream, then, as $\hat{x} \to \infty$, $S \to \infty$ for the nozzle, implying that $p, \rho \to 0$, $u(\hat{x}) \to O(1)$ and the effective Mach number $M(\hat{x}) \to \infty$; in particular, $\rho \sim S^{-1}$ and $p \sim S^{-\gamma}$. The transverse pressure gradient, negligible above, can start to re-enter the reckoning at large $\hat{x}$ however, since the representative value of $(\rho u v_x)/(p_y)$ increases as $(\beta^2\hat{x}^{-2})/(S^{-\gamma-1})$ (we use (3.2a) to provide the estimate $\hat{v} \approx S\hat{x}^{-1}$), i.e. transverse momentum becomes significant downstream when $x = \beta^{-1}\hat{x}$ is $O(S^{\frac{1}{2}(\gamma+1)})$. The same estimate comes from examining where $M\tau$ becomes $O(1)$, with $\tau \equiv \beta \mathrm{d}S/\mathrm{d}\hat{x}$ being the nozzle slope. The thin compressible boundary layer, meanwhile, has a thickness which is of order $Re^{-\frac{1}{2}}$ for x of order unity but expands in a similarity form like $x^{\frac{1}{2}}S^{\frac{1}{2}\gamma}$ downstream due to the increasing Mach number there (see Stewartson 1964). Consequently, the boundary-layer and inviscid-core thicknesses become comparable when $Re^{-\frac{1}{2}}x^{\frac{1}{2}}S^{\frac{1}{2}\gamma} \approx S$, or $x \approx Re\, S^{2-\gamma}$. Comparing this estimate with the previous, purely inviscid, estimate, we have the result that the viscous–inviscid interaction stage of interest downstream arises when

$$\Delta \approx Re^{2/3(\gamma-1)}, \tag{3.3}$$

where Δ denotes the typical nozzle width S downstream.

The farfield stage, as a result, is one of strong hypersonic viscous–inviscid interaction. The streamwise and lateral scales are of the respective orders defined by

$$[x, y, S] \rightarrow [\Delta^{\frac{1}{2}(\gamma+1)}x, \Delta y, \Delta S] \tag{3.4}$$

and the flow solution in the inviscid core acquires the form

$$[u-u_c, v, p, \rho, \psi] \approx O[\Delta^{1-\gamma}, \Delta^{\frac{1}{2}(1-\gamma)}, \Delta^{-\gamma}, \Delta^{-1}, 1], \tag{3.5}$$

while in the boundary layer, which now has thickness comparable with that of the core,

$$[u, v, p, \ldots] \approx O[1, \Delta^{\frac{1}{2}(1-\gamma)}, \Delta^{-\gamma}, \ldots]. \tag{3.6}$$

Here the constant u_c in (3.5) can be renormalized to unity.

It is interesting that this stage is analogous to the external-flow régime discussed in the preceding section, but with some important differences. The core, which is equivalent to the ISL although here there is as yet no shock present, has the nonlinear governing equations

$$\partial\rho/\partial x + \partial(\rho v)/\partial y = 0, \tag{3.7a}$$

$$\rho(\partial v/\partial x + v\,\partial v/\partial y) = -\partial p/\partial y, \tag{3.7b}$$

$$p = K\rho^{\gamma}, \tag{3.7c}$$

where (3.7c), with K constant, results from integration along the inviscid streamlines coming from upstream, cf. (2.5c). The viscous boundary layer or VSL between the core and the nozzle wall is controlled by the viscous hypersonic equations in (2.3a–f), subject again to (2.3g, h), in effect, upon renormalization. In fact these are reduced to the form

$$u = \frac{\partial\psi}{\partial y^*}, \quad u\frac{\partial u}{\partial x} - \frac{\partial\psi}{\partial x}\frac{\partial u}{\partial y^*} = -\frac{(\gamma-1)}{2\gamma p}(2H-u^2)\,p' + \gamma Cp\frac{\partial^2 u}{\partial y^{*2}}, \tag{3.8a, b}$$

$$u\frac{\partial H}{\partial x} - \frac{\partial\psi}{\partial x}\frac{\partial H}{\partial y^*} = \gamma Cp\frac{\partial^2 H}{\partial y^{*2}}, \tag{3.8c}$$

(with $u \rightarrow 1$, $H \rightarrow \frac{1}{2}$ as $y^* \rightarrow \infty$) after the HD transformation, for a unit Prandtl number.

The main differences from the external flow case earlier are two-fold, apart from the simplification in (3.7c). First, shocks are absent in this internal motion, at least for an $O(1)$ scaled distance downstream (see below), and so the number of major unknowns is reduced. The shock conditions at the unknown top of the ISL are replaced by symmetry constraints along the known symmetry line in the internal case. Further, the core-flow problem can be expressed as a nonlinear second-order wave equation whose solution subject to the above constraints is obtainable by the method of characteristics in principle. The second difference here concerns upstream influence in the interactive system. Upstream influence appears to be completely absent, according to an investigation in similar vein to that in §2. The same conclusion is found if the body shape $f(x)$ in §2 is taken to be sufficiently large, of the

PHILOSOPHICAL TRANSACTIONS OF THE ROYAL SOCIETY A MATHEMATICAL, PHYSICAL & ENGINEERING SCIENCES

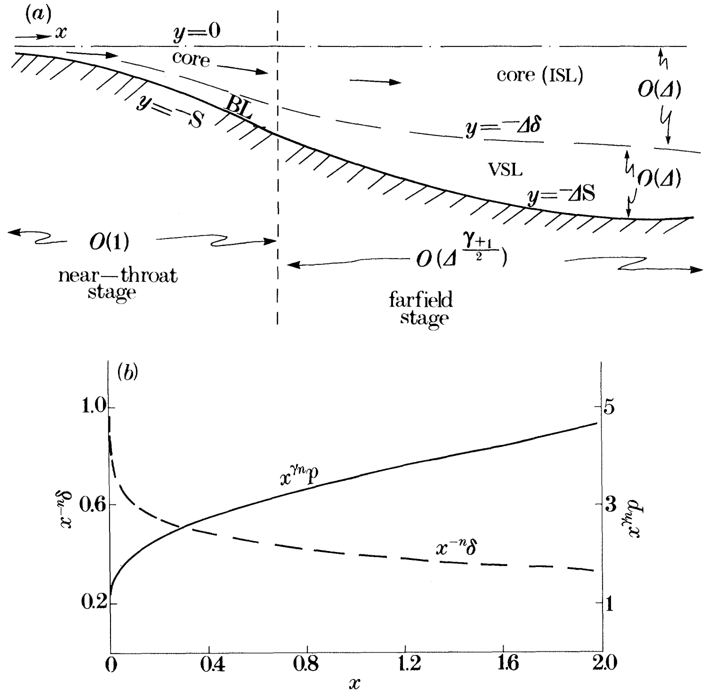

Figure 2. Hypersonic motion through a nozzle. (*a*) The two-stage flow structure, (*b*) computational results for p, δ against x, for the shape $S = x^n$, $n = 0.6$, wall enthalpy 0.4, $C = 1$, slender core, in the farfield stage.

order $x^{\frac{3}{4}}$, but negative, corresponding more to the present geometry. Hence this again reduces the computational complexity, in principle at least, since forward-marching techniques can be applied to (3.7), (3.8) from the start at $0+$. The starting solution there is of similarity form in both the core and the viscous layer, but the latter is then relatively thin and hence the interaction weak, which again contrasts with the external case, (2.6). Further, it is found that the simple VSL similarity start requires $n < 1/\gamma$, where $S \propto x^n$ near $0+$, whereas the ISL start, as posed, requires n larger, exceeding $2/(\gamma+1)$, a starting difficulty which is absent, however, for slender-flow cores with zero $\partial p/\partial y$ (see below). Strong interaction then comes in as x increases, and it seems likely that shocks and/or upstream influence, absent at the start, will appear at some finite x-location downstream. Their determination is felt to be of most concern, together with the surface shear stress and heat transfer and the pressure variation downstream. This farfield strong-interaction stage is therefore being tackled computationally at present (see figure 2). There are also limits of theoretical and practical interest, concerning either a slender-flow core or a relatively thin viscous layer, the axisymmetric version, which follows readily, the full 3D form, which is much more difficult to treat accurately, and diffuser flows associated with contraction of the nozzle width downstream.

4. Hypersonic instability and transition studies

There are numerous aspects to the instability and transition of hypersonic boundary layers and shock layers, and some of these are being addressed as described below.

The first starts with the viscous instability of compressible boundary layers. The main previous work in this area is based on Orr–Sommerfeld linear parallel-flow theory (see, for example, Mack 1984; Malik 1987), and is of much interest, but its neglect of non-parallel flow effects is necessarily regarded as questionable, especially at higher Mach numbers as the boundary layer becomes more and more non-parallel. This leads to the recent asymptotic approach of Smith (1987*a*), where the viscous or Tollmien–Schlichting (TS) theory is put on a rational basis by means of triple-deck arguments, for linear or nonlinear TS disturbances. Thus the unsteady viscous–inviscid interactive system, in scaled variables, controlled by the 3D interactive boundary-layer equations

$$U_X + V_Y + W_Z = 0, \tag{4.1a}$$

$$U_{\hat{t}} + UU_X + VU_Y + WU_Z = -P_X + U_{YY}, \tag{4.1b}$$

$$W_{\hat{t}} + UW_X + VW_Y + WW_Z = -P_Z + W_{YY}, \tag{4.1c}$$

$$U = V = W = 0 \quad \text{at} \quad Y = 0, \tag{4.1d}$$

$$U \sim Y + A(X, Z, \hat{t}), \quad W \to 0 \quad \text{as} \quad Y \to \infty, \tag{4.1e}$$

is applied, coupled with the compressible potential-flow behaviour holding just outside the boundary layer and satisfying

$$\left[(M_\infty^2 - 1)\left(\frac{\partial^2}{\partial X^2} \mp \frac{\partial^2}{\partial \bar{y}^2}\right) - \frac{\partial^2}{\partial Z^2}\right]\bar{p} = 0, \tag{4.1f}$$

$$\bar{p} \to 0 \text{ (or outgoing waves)} \quad \text{as} \quad \bar{y} \to \infty, \tag{4.1g}$$

$$\bar{p} \to P, \quad \bar{p}_{\bar{y}} \to A_{XX}, \quad \text{as} \quad \bar{y} \to 0+, \tag{4.1h}$$

for $M_\infty \gtrless 1$. Here the pressure P and the displacement $-A$ are both unknown functions of $X, Z, \hat{t}$, and 3D linear or nonlinear instability properties are of interest. The linearized version, where $U - Y$, $V, W, P, A, \bar{p}$ are all relatively small, produces results (Smith 1989) that agree fairly well with the previous Orr–Sommerfeld computations, at least at moderate M_∞ values. As M_∞ increases the agreement diminishes, and this seems almost certainly due to the neglect of nonparallel-flow effects in the previous work; in fact Smith (1989) shows that the parallel-flow approximation can hold only if the Mach number is much less than the size

$$M_\infty = O(Re^{\frac{1}{10}}), \tag{4.1i}$$

a restriction which seems in line with the comparisons above. Another restriction on the TS waves is that they must be directed outside of the wave-Mach-cone, in the hypersonic régime, i.e. be effectively subsonic waves (see figure 3). Further studies in this area are by Bowles & Smith (1989), Cowley & Hall (1990) and Blackaby (1991), who addresses the stage (4.1*i*) which corresponds to the viscous instability modes becoming completely non-parallel flow ones.

The full nonlinear unsteady problem (4.1) is of most interest with regard to transition, however, and its properties are being considered from several standpoints. Thus vortex-wave interactions implied by (4.1) are discussed in Smith & Walton (1989) and Walton (1991), while full computations are given in Smith (1991), albeit for the incompressible 3D case. Both the vortex-wave phenomenon and the full triple-deck response are powerful unsteady processes at any Mach number, leading to complete alteration of the mean-flow profile from its original steady shape. The vortex-wave case (Smith & Walton 1989; Hall & Smith 1989) involves TS-like waves

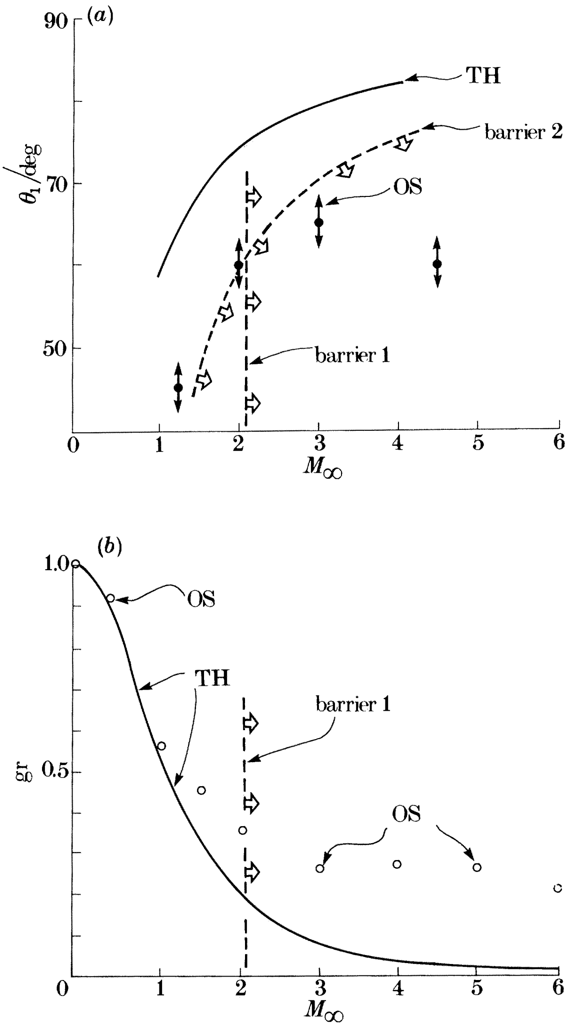

Figure 3. Comparisons and restrictions concerning the viscous–inviscid first-mode instability in an insulated boundary layer, taken from Smith (1989). TH, OS denote theoretical asymptotic and Orr–Sommerfeld results respectively; (*a*) for the angle (θ_1) of maximum spatial growth rate, (*b*) for the normalized maximum spatial growth rate (gr). 'Barrier 1, 2' stand for the restrictions $M_\infty \ll Re^{\frac{1}{10}}$ (' $\ll$ ' is replaced here by ' $< \frac{1}{2}$', and see (4.1 *i*)) and $\tan\theta_1 > (M_\infty^2 - 1)^{\frac{1}{2}}$ (wave-Mach-cone) on the OS computations, with the open arrows indicating regions of invalidity of the OS approach.

which are relatively small but of sufficiently fast streamwise scales that they are able to interact with the large-amplitude but slower-scale vortex motion induced, leaving the two components inter-dependent. Strong vortex structures can thereby be provoked within the boundary layer. We note also the properties of surface cooling mentioned below. The full triple-deck case (4.1) on the other hand can lead to a nonlinear localized break-up of the flow solution within a finite time (Smith 1988; see also comparisons by Walker 1990), a process which is believed to be connected with intermittency ultimately, and brings about a substantial change in the scales and unsteady flow structure locally. In particular, normal pressure gradients are brought into play via a predominantly inviscid region surrounding the break-up position, and the surface shear stress locally is increased by an order of magnitude, as is the streamwise pressure gradient. Work continuing in this area is by Hoyle *et al.* (1991).

Secondly, there is the inviscid instability of the compressible boundary layer to consider, at large Mach numbers. The inviscid modes are many, and they are governed by the compressible Rayleigh equation for the pressure perturbation $\tilde{p}$,

$$\tilde{p}'' - (2\bar{M}'/\bar{M})\,\tilde{p}' - \alpha^2(1-\bar{M}^2)\,\tilde{p} = 0 \tag{4.2}$$

at finite Mach numbers, with α, c being the unknown wavenumber and wavespeed respectively and $\bar{M} \equiv (\bar{u}-c)M_\infty/\bar{T}^{\frac{1}{2}}$, where $\bar{u}$ and $\bar{T}$ are the basic velocity and temperature profiles in turn. Computations of (4.2), with $\tilde{p}'(0), \tilde{p}(\infty)$ zero typically, are due principally to Mack (1984) and Malik (1987), although there are numerous other related computations for various conditions. At large Mach numbers the instability modes develop into two main kinds (Smith & Brown 1990), a single so-called vorticity mode having the major growth rate and a host of so-called acoustic modes with relatively minor growth rates. The vorticity mode (Smith & Brown 1990) is concentrated spatially near the edge of the hypersonic boundary layer, in a comparatively thin region, and has the property that α increases logarithmically with the Mach number, for the Blasius case, specifically

$$\alpha \approx \bar{\alpha}(\ln M_\infty^2)^{\frac{1}{2}}, \quad c-1 = O(M_\infty^{-2}). \tag{4.3a,b}$$

For example, the neutral case has $\bar{\alpha} = \frac{1}{4}$; and the maximum growth rate αc_i, of order $M_\infty^{-2}(\ln M_\infty^2)^{\frac{1}{2}}$, is captured within the régime (4.3) (see also figure 4). The acoustic modes (Smith & Brown 1990; Cowley & Hall 1990), on the other hand, typically span the whole boundary layer and have α decreasing with the Mach number, with the scales

$$\alpha = O(M_\infty^{-2}), \quad c-1 = O(M_\infty^{-2}), \tag{4.4a,b}$$

where the leading-order terms are neutral, leaving growth rates αc_i only of order $M_\infty^{-6}(\ln M_\infty^2)^{-\frac{1}{2}}$. These solutions are discussed by Smith & Brown (1990) along with an examination of two extra features of note, namely the near mode-crossing present and the possible creation of low-wavenumber outgoing waves at sufficiently large M_∞ values. The near mode-crossing, which is increasingly evident in Mack's (1984) computations at increasing Mach number, corresponds to the vorticity-mode branch of (4.3) being an almost, but not quite, continuous curve in the αM_∞ plane. The discontinuities, or switches in mode number, are exponentially small at large M_∞. This prediction, and those of (4.3), (4.4), agree qualitatively and sometimes quantitatively with the computations mentioned above, and there is also broader application, e.g. to free shear layers and wakes (see figure 4). Extra properties of the growth rates at large M_∞ are being studied by S.N.B.

Surface-cooling effects on the inviscid modes are considered in Seddougui *et al.* (1989), although it turns out (see same reference) that the cooling effect is in some senses much more pronounced in the viscous-mode TS response, producing surprisingly large spatial growth rates. Surface cooling, which is often vital in real hypersonic flight, provokes a near square-root behaviour in the velocity and temperature profiles close to the surface, and hence the skin friction and heat transfer are enhanced. As a result, for supersonic or hypersonic boundary layers, the cooling tends to shorten the TS length and time scales, leading to a novel form of viscous–inviscid interaction in which (4.1*a*–*e*) hold but with a *P*–*A* relation stemming from (4.2), with $c = 0$, essentially. The predictions from the last-named paper appear to be in line with the experimental findings of Lysenko & Maslov (1984). On the nonlinear

PHILOSOPHICAL TRANSACTIONS OF THE ROYAL SOCIETY A MATHEMATICAL, PHYSICAL & ENGINEERING SCIENCES

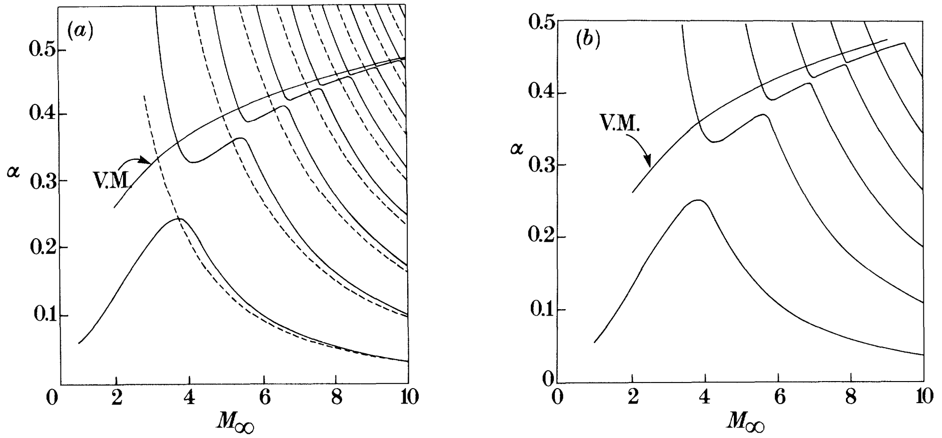

Figure 4. Comparisons, from Smith & Brown (1990), between computational solutions of (4.2) and the vorticity mode (denoted V. M.) (see (4.3)) for high Mach number, for inviscid neutral stability in (*a*) a boundary layer (also shown, dashed, are the limiting acoustic modes), (*b*) the wake of a flat plate (including sample results from Papageorgiou 1991).

side, the most obvious resort is to the unsteady compressible Euler equations, in 2D or 3D. Vortex-wave nonlinear interactions can also occur here (Hall & Smith 1989; and references therein), however, and there is a link with Hall & Fu's (1991; see also references therein) work on Görtler vortices. In the vortex-wave interactions the wave component is a modification of the compressible Rayleigh ones in (4.2)–(4.4), while the unknown basic flow is driven by a wave-amplitude-squared forcing effect close to the critical layer. This type of nonlinear interaction has many interesting points to it, especially in the hypersonic range where (4.3), (4.4) can come into operation. Some possibilities here are considered by Hall & Smith (1989) and these and others are currently being studied, there being also a possible link with Holden's (1985) experimental finding of rope-like vortex structures near the edge of a hypersonic boundary layer at approximately Mach 12.

The third aspect being studied concerns the linear and nonlinear stability of inviscid shock layers such as that discussed in §2, in the hypersonic nonlinear régime. The typical nonlinear disturbance under investigation travels downstream at the freestream speed but with a short streamwise dependence present and, in the appropriate moving frame, its governing equations are in effect those of unsteady 2D Euler flow,

$$\frac{\partial\bar\rho}{\partial x}+\frac{\partial}{\partial\xi}(\bar\rho\bar u)+\frac{\partial}{\partial\bar y}(\bar\rho\bar v)=0,\quad \bar\rho\left(\frac{\partial\bar u}{\partial x}+\bar u\frac{\partial\bar u}{\partial\xi}+\bar v\frac{\partial\bar u}{\partial\bar y}\right)=-\frac{\partial\bar p}{\partial\xi},\qquad(4.5\,a,b)$$

$$\bar\rho\left(\frac{\partial\bar v}{\partial x}+\bar u\frac{\partial\bar v}{\partial\xi}+\bar v\frac{\partial\bar v}{\partial\bar y}\right)=-\frac{\partial\bar p}{\partial\bar y},\quad \left(\frac{\partial}{\partial x}+\bar u\frac{\partial}{\partial\xi}+\bar v\frac{\partial}{\partial\bar y}\right)\left(\frac{\bar p}{\bar\rho^{\gamma}}\right)=0,\qquad(4.5\,c,d)$$

subject to four unsteady-shock conditions on top, and tangential flow at the body surface below. Here the spatial development of the disturbance is being considered, however, with ξ standing for the fast streamwise coordinate $(x-t)/\epsilon$, ϵ is of order M_∞^{-1} and

$$u=1+\epsilon\bar u+\ldots,\quad v=\epsilon\bar v+\ldots,\qquad(4.6\,a,b)$$

$$p=\gamma(\epsilon M_\infty)^2\,\bar p+\ldots,\quad \rho=\bar\rho+\ldots,\quad y=\epsilon\bar y,\qquad(4.6\,c,d,e)$$

cf. (2.4). The steady version where $\partial/\partial\xi \equiv 0$ and $\bar{u} \equiv 0$ reproduces (2.5), and small perturbations about the steady flow solution ($\bar{v}_0, \bar{p}_0, \bar{\rho}_0$, say) then produce a linearized stability system. What is surprising perhaps is that the latter system is a non-parallel flow one, despite the rapid streamwise variation with ξ. Spatially concentrated disturbances, both linear and nonlinear, are currently being considered, these being of more practical as well as theoretical interest. They are associated with increased frequencies and, if originating from the shock, they can travel downstream concentrated around the particular basic-flow streamline ($\mathrm{d}\bar{y}/\mathrm{d}x = \bar{v}_0$) or around the minus characteristic ($\mathrm{d}\bar{y}/\mathrm{d}x = \bar{v}_0 - \bar{a}_0$, where $\bar{a}_0^2 \equiv \gamma\bar{p}_0/\bar{\rho}_0$ from (2.5)) stemming from the impingement point. The governing equations found for such disturbances are very dependent on the underlying flow properties, including the induced vorticity, and are currently being studied. The collision and reflection process, for instance, occurring where the minus characteristic meets the body surface (effectively $\delta(x)$) and triggers disturbances along the plus characteristic of slope $\bar{v}_0 + \bar{a}_0$ downstream, is of much concern, as is the spatial growth induced.

Fourth is the matter of possible interactions between the instabilities of the ISL and the VSL, allowing disturbances from external shock oscillations for instance to penetrate into the VSL and perhaps amplify there. In the strong-interaction range (2.1) the VSL inviscid instability can still be controlled by the scalings and pressure equation implied by (4.4), whereas the ISL inviscid instability takes the form in (4.5), (4.6). Here the acoustic modes are being considered first rather than the vorticity mode, because their normal scales seem more likely to provoke ISL–VSL interplay. The precise form of this interplay is, again, under consideration, along with the alterations in the inner and outer conditions on the ISL and VSL stability problems respectively.

Finally, we note that the instability and transition theories summarized above apply also to thicker-body external flows and to the internal nozzle flow of §3, with appropriate modifications. These applications have still to be followed through fully, as have the influence of other temperature–viscosity laws, real-gas effects, entropy-layer effects and many other issues of interest. The emphasis, however, in the transition studies, is ultimately in the nonlinear régime throughout, where for large Mach numbers there appear to be few, if any, actual results as yet apart from the finite-time break-up mentioned in the third paragraph of this section.

Thanks are due to the Science and Engineering Research Council and to the Ministry of Defence for their joint support of much of this work, to AFOSR, ICASE and UTRC for some support, to ULCC and UCLCC for computer facilities, to Dr T. A. Holbeche for many helpful discussions on the research, and to a number of colleagues for their interest and comments.

References

Blackaby, N. D. 1991 Ph.D. thesis, University of London, U.K.

Bowles, R. I. 1990 Ph.D. thesis, University of London, U.K.

Bowles, R. I. & Smith, F. T. 1989 On boundary-layer transition in transonic flow. *Utd. Tech. Res. Center Rept.* UT89-26.

Brotherton-Ratcliffe, R. V. 1986 Ph.D. thesis, University of London, U.K.

Brown, S. N., Cheng, H. K. & Lee, C. J. 1990 Inviscid–viscous interaction on triple-deck scales in a hypersonic flow with strong wall cooling. *J. Fluid Mech.* **220**, 309–337.

Brown, S. N., Stewartson, K. & Williams, P. G. 1975 Hypersonic self-induced separation. *Phys. Fluids* **18**, 633–639.

Carter, J. E. 1979 A new boundary layer inviscid iteration technique for separated flows. *AIAA paper no. 79-1450*.

Cowley, S. J. & Hall, P. 1990 On the instability of hypersonic flow past a wedge. *J. Fluid Mech.* **214**, 17–42.

Davis, R. T. 1984 A procedure for solving the compressible interacting boundary-layer equations for subsonic and supersonic flows. *AIAA paper no. 84-1614*.

Hall, P. & Fu, Y. 1991 *Theor. Comp. Fluid Dyn.* (In the press.)

Hall, P. & Smith, F. T. 1989 On strongly nonlinear vortex/wave interactions in boundary-layer transition. *ICASE Rept. 89-82*. (Also *Euro. J. Mech.* B **8**, 179–205 (1989) and *J. Fluid Mech.* (Submitted.).)

Holden, M. S. 1985 *AIAA paper no. 85-0325*.

Hoyle, J. M., Smith, F. T. & Walker, J. D. A. 1991 Sublayer eruption and vortex formation. *Comp. Phys. Commun.* (In the press.)

Khorrami, A. F. 1991 D.Phil. thesis, University of Oxford, U.K.

Khorrami, A. F. & Smith, F. T. 1991 (In preparation.)

Lysenko, V. I. & Maslov, A. A. 1984 The effect of cooling on supersonic boundary-layer stability. *J. Fluid Mech.* **147**, 39–52.

Mack, L. M. 1984 Boundary layer linear stability theory. *AGARD Rept. 709*. (Also *AIAA J.* **13**, 278–289 (1975).)

Malik, M. R. 1987 Prediction and control of transition in hypersonic boundary layers. *AIAA paper no. 87-1414*. (Also *NASA CR-165925* (1982).)

Neiland, V. Ya. 1970 Upstream propagation of disturbances in hypersonic boundary layer interactions. *Izv. Akad. Nauk. SSSR, Mekh. Zhid. i Gaza* **4**, 40–49.

Papageorgiou, D. T. 1991 (In preparation.)

Rizzetta, D. P., Burggraf, O. R. & Jenson, R. 1978 Triple-deck solutions for viscous supersonic and hypersonic flow past corners. *J. Fluid Mech.* **89**, 535–552.

Seddougui, S. O., Bowles, R. I. & Smith, F. T. 1989 Surface-cooling effects on compressible-boundary-layer instabilities and upstream influence, *ICASE Rept. 89*. (Also *Euro. J. Mech.* (In the press.).)

Smith, F. T. 1988 Finite-time break-ups can occur in any unsteady interactive boundary layer. *Mathematika* **35**, 256–273.

Smith, F. T. 1989 On the first-mode instability in subsonic, supersonic and hypersonic boundary layers. *J. Fluid Mech.* **198**, 127–153.

Smith, F. T. 1991 Steady and unsteady 3D interactive boundary layers. *Computers Fluids*. (In the press.)

Smith, F. T. & Brown, S. N. 1990 The linear inviscid instability of a Blasius boundary layer at large values of the Mach number. *J. Fluid Mech.* **219**, 499–518.

Smith, F. T. & Gajjar, J. S. B. 1983 On hypersonic self-induced separation, hydraulic jumps and boundary layers with algebraic growth. *Mathematika* **30**, 77–93.

Smith, F. T. & Khorrami, A. F. 1991 The interactive breakdown in supersonic ramp-flow. *J. Fluid Mech.* (In the press.)

Smith, F. T. & Walton, A. G. 1989 Nonlinear interaction of near-planar TS waves and longitudinal vortices in boundary-layer transition. *Mathematika* **36**, 262–289.

Stewartson, K. 1964 *Theory of laminar boundary layers in compressible fluids*. Oxford University Press.

Stewartson, K. & Williams, P. G. 1973 Self-induced separation II. *Mathematika* **20**, 98–108.

Walker, J. D. A. 1990 The structure of an erupting boundary layer. In *Proc. Workshop on Unsteady Separation*. Ohio State University.

Walton, A. G. 1991 Ph.D. thesis, University of London, U.K.

Werle, M. J., Dwoyer, D. L. & Hankey, W. L. 1973 *AIAA J.* **11**, 525.